Smart Structures and Systems, *Vol. 23, No. 3 (2019) 295-306*
DOI: https://doi.org/10.12989/sss.2019.23.3.295

Investigation of the SHM-oriented model and dynamic characteristics of a super-tall building

Hai-Bei Xiong[1], Ji-Xing Cao[1], Feng-Liang Zhang[*2,1], Xiang Ou[3] and Chen-Jie Chen[4]

[1]*Department of Disaster Mitigation for Structures, Tongji University, 1239 Siping Road, Shanghai, China*
[2]*School of Civil and Environmental Engineering, Harbin Institute of Technology (HIT), Shenzhen, China*
[3]*East China Region of Tahoe (Group) Co. Ltd., Shanghai, China*
[4]*Shanghai Architectural Design & Research (Co., Ltd.), Shanghai, China*

(Received May 27, 2018, Revised November 1, 2018, Accepted November 14, 2018)

Abstract. Shanghai Tower is a 632-meter super high-rise building located in an area with wind and active earthquake. A sophisticated structural health monitoring (SHM) system consisting of more than 400 sensors has been built to carry out a long-term monitoring for its operational safety. In this paper, a reduced-order model including 31 elements was generated from a full model of this super tall building. An iterative regularized matrix method was proposed to tune the system parameters, making the dynamic characteristic of the reduced-order model be consistent with those in the full model. The updating reduced-order model can be regarded as a benchmark model for further analysis. A long-term monitoring for structural dynamic characteristics of Shanghai Tower under different construction stages was also investigated. The identified results, including natural frequency and damping ratio, were discussed. Based on the data collected from the SHM system, the dynamic characteristics of the whole structure was investigated. Compared with the result of the finite element model, a good agreement can be observed. The result provides a valuable reference for examining the evolution of future dynamic characteristics of this super tall building.

Keywords: super high-rise building; reduced-order model; regularization matrix method; dynamic characteristics; modal identification

1. Introduction

As large-scale structures have developed rapidly in the past few decades, the safety and serviceability of these structures are the main concerns during the whole life-cycle stage (Cao and Li 2019, Yi *et al.* 2013, Ni *et al.* 2012, Zhang *et al* 2017). Structure health monitoring systems can monitor structural response, loads and environmental effects through various sensors, providing good solutions to the evaluation of structure. Successful applications of the SHM systems to large-scale structures have been widely reported. For example, to monitor the static and dynamic characteristics of a skyscraper Burj Khalifa in Dubai, an extensive SHM program was installed to evaluate the structural performance, to control the construction process and to investigate the correlation between the measured and predicted behavior (Abdelrazaq *et. al* 2012). A complex SHM system consisting of more than 800 sensors was instrumented in the Canton Tower in a continuous and long term manner, and the structural performance under various events was evaluated (Ni *et al.* 2009). There were more than 150 buildings in California, USA (Kijewski-Correa *et al.* 2003) and more than 100 buildings in Japan (Huang *et al.* 2006) instrumented with strong motion monitoring systems to investigate the earthquake-induced response.

∗Corresponding author, Ph.D.
E-mail: fengliangzhang@hotmail.com

Accompanied with a large quantities of field data from the SHM program, modal identification technique played an important role in the evaluation of dynamic characteristics (Au 2017). Osmancikli *et al.* identified the natural frequencies, mode shapes and modal damping ratios of a historical masonry bell-tower, and these parameters were used to evaluate the structural performance for both pre-restored and restored cases (Osmancikli *et al.* 2012). Chen *et al.* adopted the enhanced frequency domain decomposition method and the stochastic subspace identification method to identify the dynamic characteristics of a 600-meter height structure (Chen *et al.* 2011). Recently, Bayesian modal identification approach aroused many researchers' interest (Ni *et al.* 2016, Yin *et al.* 2017, Au 2017, Ng *et al.* 2018, Ni and Zhang 2018, 2019). Zhang *et al.* utilized a fast Bayesian FFT method to identify modal properties of the Canton Tower using ambient vibration data (Zhang *et al.* 2016a). Li *et al.* proposed variational Bayes method to obtain the posterior distributions of modal parameters and it was illustrated by the application to a mass-spring system and a high-rise building (Li *et al.* 2017).

By applying modal identification techniques to real-life data, assessments for large-scale structures have been extensively carried out (Au *et al.* 2012, Ni and Zhang 2016, Ni *et al.* 2017, Xiong *et al.* 2018, Zhang *et al.* 2018, Ni *et al.* 2019). Yi *et al.* compared the accuracy of displacement determined by GPS and accelerometers using the in-situ data of a super-tall building during five typhoons, and investigated the amplitude-dependent characteristics of

http://www.techno-press.com/journals/sss&subpage=7 ISSN: 1738-1584 (Print), 1738-1991 (Online)

damping ratios (Yi *et al.* 2013). Guo *et al.* employed different techniques to identify the modal properties, to investigate the amplitude-dependence behavior of modal properties, and to evaluate the serviceability and comfort during different typhoon events (Guo *et al*. 2012). Rahmani *et al.* hosted a 54-story steel-frame building as a benchmark to investigate the variations of identified wave velocities of vertically propagating waves using records during six earthquakes over a period of 19 years (Rahmani *et al.* 2015). The aforementioned work observed some interesting trends under various extreme events, providing a database for the future condition assessments and design guidance.

For large-scale structures, fast analysis or even real-time monitoring tended to be necessary for SHM program as it was capable of providing an early warning if an extreme event happened. In general, a sophisticated finite element (FE) model (FE model) usually took a long time to calculate the structural response, while a reasonable reduced-order model (ROM) for a large-scale structure can calculate the response more efficiently, which was helpful to alleviate the computational burden and provided an orthogonality check for analytical and experimental results. The ROM was also useful in model updating (Au and Zhang 2016). The most popular reduction method was static Guyan's reduction (Downs 1980) and the improved reduced system method (Flanigan 1991). Recently, the proper orthogonal decomposition method has been developed to generate a ROM by using a given set of input forces for the full model (Kerschen *et al.* 2005). Amabili proposed a rigorous method for interpolating a set of parameterized linear structural dynamics ROM, without operating on the underlying set of parameterized full model (Amabili *et al.* 2003). A quadratic manifold approach was proposed to establish the ROM featuring geometric nonlinearities (Jain *et al.* 2017, Rutzmoser *et al.* 2017). Although various methods were developed to establish the ROM, most of them were only verified with small-size structures or numerical simulations, while the ROM for a large-scale structure may accompany ill-conditioned and robustness problems.

In this paper, a regularization method was adopted to solve the ill-condition problem encountered in the existing model tuning method and it was demonstrated by a large-scale structure-Shanghai Tower to determine the ROM of the structure from a sophisticated FE model. Based on the SHM system installed on Shanghai Tower, the dynamic characteristics of this super tall building were also investigated during the construction and service stages. The outline was as follows: in Section 2, taking the Shanghai Tower as a host structure, the procedure of a ROM generated from a sophisticated FE model was presented. In Section 3, an iterative matrix algorithm with regularization was proposed to narrow the gap between the ROM and the full model. In Section 4, the result of long-term monitoring for Shanghai Tower under different construction and in-service stages was presented and the possible trend of modal parameters including natural frequencies and damping ratios were discussed.

2. The reduced-order model of Shanghai Tower

Shanghai Tower is located in Lujiazui District (Fig. 1), Shanghai, China. A tapering shape with consistently rounded corners is designed to reduce the lateral loads. A special structure system, mega-frame core-wall structural system, is adopted to resist the lateral loads. Along the height, the structure is divided into nine zones, each of which includes 12 to 15 floors. There is a strengthened floor between two different zones, and it is regarded as safety refuge areas if the emergency accident happens. The diameter of the structural plane gradually decreases from 83.6 meters at the bottom zone to 42.0 meters in the eighth zone. A three-dimensional FE model for Shanghai Tower was built using ETABS (Fig. 2), to simulate the structural performance under various loading.

The full model of Shanghai Tower was so complicated that it took much time to complete the calculation. A procedure for ROM generating from the full model was developed. The main idea was that the stiffness of the ROM was attached to an element based on stiffness equivalent principle and the corresponding mass was lumped to a node. Fig. 3 showed a sketch of the ROM consisting of 31 elements. The part of steel truss at the top of the building was not taken into consideration. For each element, six degrees of freedom (DOFs) were considered, including three horizontal translational DOFs and three rotational DOFs. Table 1 showed the detailed information of elements.

Fig. 1 View of Shanghai Tower

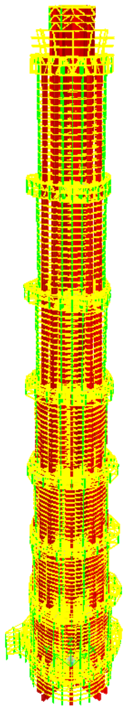

Fig. 2 FE model established by ETABS

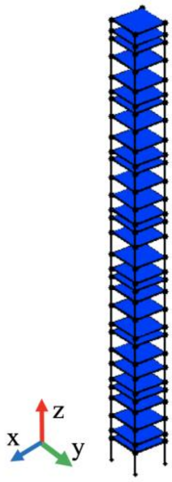

Fig. 3 A sketch of ROM

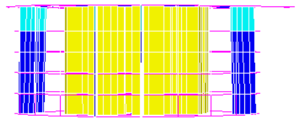

(a)An element of 3D

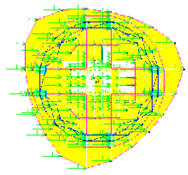

(b)A unit displacement imposed for *x* direction on the upper section

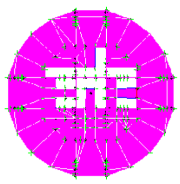

(c) Six DOFs at the bottom section fixed

Fig. 4 Form an element' stiffness of ROM

Table 1 Element information of the ROM

Element ID	Element length/m	Element ID	Element length/m	Element ID	Element length/m
1	14.5	12	22.5	23	23.3
2	9.9	13	19	24	18
3	22.5	14	9.9	25	19
4	25.8	15	18.8	26	9.9
5	18.4	16	27	27	14.3
6	9.9	17	19	28	22.5
7	22.5	18	9.9	29	19
8	25.8	19	14.3	30	9.9
9	18.4	20	22.5	31	28.9
10	9.9	21	23.5		
11	23.3	22	9.9		

A detailed illustration about how to form the stiffness matrix of an element was presented in Fig. 4. A node for ROM was taken from the corresponding segment in full model (Fig. 4(a)). A unit displacement was imposed on one DOF of the upper section, i.e., x direction was imposed while the other directions were constrained (Fig. 4(b)). At the same time, all the six DOFs of the lower section were fixed (Fig. 4(c)). Hence, the generalized force was equivalent to the corresponding column of the element stiffness matrix, i.e., the first column in an element stiffness matrix. When all the six DOFs of an element sequentially followed to the above procedure, an element stiffness matrix can be formed. When the stiffness matrices for all elements were calculated, a global stiffness matrix for ROM can be assembled.

Table 2 Floors information of the ROM

Node ID	Floor elevation/ m	Node ID	Floor elevation/ m	Node ID	Floor elevation/ m
1	561	12	360.1	23	163.8
2	546.5	13	337.6	24	140.5
3	536.6	14	318.6	25	122.5
4	514.1	15	308.7	26	103.5
5	488.3	16	289.9	27	93.6
6	469.9	17	262.9	28	79.3
7	460	18	243.9	29	56.8
8	437.5	19	234	30	37.8
9	411.7	20	219.7	31	27.9
10	393.3	21	197.2		
11	383.4	22	173.7		

For an element matrix, the equivalent mass was lumped to a node. Table 2 showed the information of nodes. Since the node mass was assigned to the nearest nominal section center in the full model, the equivalent mass and moment of inertia of an element were calculated by Eq. (1)

$$\begin{aligned} m_e &= \sum_{i=1}^{n} m_i \\ I_r &= \sum_{i=1}^{n} m_i r_i^2 \end{aligned} \tag{1}$$

where m_e was the equivalent mass of each element for ROM; I_r was the equivalent moment of inertia for each element; n was the total number of nodes for a corresponding element in the full model; m_i was the node ith mass in the full model; r_i was the projection distances between node ith and the nearest nominal section center. After the mass matrix for all elements were obtained and they were assembled to a global mass matrix for ROM.

As the ROM was simplified based on the equivalent stiffness of components, the response of this model was not sensitive at element and material levels. As a result, it was difficult to exactly locate where the damage happened when the mode parameters changed during the structure health monitoring. In general, the obtained ROM can be used for fast analysis in linear case, providing an orthogonality for analytical and experimental results. To calibrate the ROM and make the prediction more reliable, a regularization method was proposed to tune the ROM in the next section.

3. Regularization matrix method for tuning the reduced-order model

3.1 A regularization matrix method

For an N DOFs structure, the eigenvalue equation can be written as

$$[\mathbf{K}_R - \boldsymbol{\omega}_R^2 \boldsymbol{M}_R]\boldsymbol{\Phi}_R = 0 \tag{2}$$

where $\boldsymbol{K}_R$ and $\boldsymbol{M}_R$ were respectively global stiffness matrix and global mass matrix of the ROM; $\boldsymbol{\omega}_R$ and $\boldsymbol{\Phi}_R$ were respectively the natural frequency and corresponding mode shapes of the ROM. Note that all the mode shape vectors in this work were normalized to 1.

System parameters were used to tune the modal parameters, e.g., stiffness matrix and mass matrix. The perturbations of the structural stiffness matrix and mass matrix were defined as

$$\begin{cases} \widetilde{\boldsymbol{K}} = \boldsymbol{K}_R + \Delta\boldsymbol{K} \\ \widetilde{\boldsymbol{M}} = \boldsymbol{M}_R + \Delta\boldsymbol{M} \end{cases} \tag{3}$$

where $\widetilde{\boldsymbol{K}}$ and $\widetilde{\boldsymbol{M}}$ denoted the global stiffness matrix and global mass matrix of the tuned ROM, respectively; $\Delta\boldsymbol{K}$ and $\Delta\boldsymbol{M}$ were the perturbations of stiffness and mass matrix between the initial ROM and the tuned ROM, respectively.

Similarly, the eigenvalue equation for the tuned model can be expressed as

$$[\widetilde{\boldsymbol{K}} - (\boldsymbol{\omega}^*)^2 \widetilde{\boldsymbol{M}}]\boldsymbol{\Phi}^* \approx 0 \tag{4}$$

where $\boldsymbol{\omega}^*$ and $\boldsymbol{\Phi}^*$ were the natural frequency and corresponding mode shapes matrix from full model, respectively.

When substituting Eq. (3) into the Eq. (4), and putting the unknown matrixes together, the governing equations can be given by

$$[\boldsymbol{\Delta K}, \boldsymbol{\Delta M}]\begin{pmatrix} \boldsymbol{\Phi}^* \\ -(\omega^*)^2\boldsymbol{\Phi}^* \end{pmatrix} = ((\omega^*)^2\boldsymbol{M_R} - \boldsymbol{K_R})\boldsymbol{\Phi}^* \tag{5}$$

Actually the system of linear equation in Eq. (5) usually cannot be determined, depending on the available number of modal parameters $\boldsymbol{\omega}^*$, $\boldsymbol{\Phi}^*$. Assuming there were mth orders available, Eq. (5) can be expanded as follows

$$\begin{aligned} &[\boldsymbol{\Delta K}, \boldsymbol{\Delta M}]\begin{pmatrix} \emptyset_1^* & \emptyset_2^* & \cdots & \emptyset_m^* \\ -(\omega_1^*)^2\emptyset_1^* & -(\omega_2^*)^2\emptyset_2^* & & -(\omega_m^*)^2\emptyset_m^* \end{pmatrix} = \\ &[((\omega_1^*)^2\boldsymbol{M_R} - \boldsymbol{K_R})\emptyset_1^* \quad ((\omega_2^*)^2\boldsymbol{M_R} - \boldsymbol{K_R})\emptyset_2^* \quad \dots \quad ((\omega_m^*)^2\boldsymbol{M_R} - \boldsymbol{K_R})\emptyset_m^*] \end{aligned} \tag{6}$$

where ω_k^* was the kth frequency and $\emptyset_k^*$ was the corresponding kth mode shape $(k = 1,2,\cdots,m)$.

In Eq. (6), $[\boldsymbol{\Delta K}, \boldsymbol{\Delta M}]$ contained $N \times 2N$ unknown parameters and each row was independent according to the matrix multiplication law. Hence, it was decomposed into N individual equations. Each equation contained $2N$ unknown parameters, which can be constructed as

$$\mathbf{A}\boldsymbol{x}=\mathbf{b}$$

where $\mathbf{A} = \begin{pmatrix} \emptyset_1^* & \emptyset_2^* & \cdots & \emptyset_m^* \\ -(\omega_1^*)^2\emptyset_1^* & -(\omega_2^*)^2\emptyset_2^* & & -(\omega_m^*)^2\emptyset_m^* \end{pmatrix}^{\mathrm{T}}$; $\boldsymbol{x} = [\Delta K_j, \Delta M_j]^{\mathrm{T}}$;

$$\mathbf{b} = \begin{pmatrix} \left[\left((\omega_1^*)^2\mathbf{M_R} - \mathbf{K_R}\right)_j \emptyset_1^*\right]^{\mathrm{T}} \\ \left[\left((\omega_1^*)^2\mathbf{M_R} - \mathbf{K_R}\right)_j \emptyset_2^*\right]^{\mathrm{T}} \\ \vdots \\ \left[\left((\omega_1^*)^2\mathbf{M_R} - \mathbf{K_R}\right)_j \emptyset_m^*\right]^{\mathrm{T}} \end{pmatrix} \tag{7}$$

where $\Delta K_j, \Delta M_j$ were the jth row of matrix $\boldsymbol{\Delta K}$ and $\boldsymbol{\Delta M}$ $(j = 1, 2, \cdots, N)$.

Performing the singular value decomposition (SVD) of $\mathbf{A}$, the following equation can be obtained

$$\mathbf{A}_{(m\times N)} = \mathbf{U}_{(m\times m)} \sum\nolimits_{(m\times N)} \mathbf{V}_{(N\times N)}^{\mathrm{T}} = \sum\nolimits_{j=1}^{m} \sigma_j u_j v_j^T \tag{8}$$

where $\sum$ was a diagonal matrix containing singular values σ_j. The orthonormal column vector u_j in $\boldsymbol{U}$ and v_j in $\boldsymbol{V}$ were the left and right singular vectors, respectively. Therefore, the solution of Eq. (7) can be formulated as

$$x = \sum\nolimits_{j=1}^{m} \frac{u_j^T b}{\sigma_j} v_j \tag{9}$$

In general, the relationship between system parameters and their dynamic response was nonlinear, so an iteration approach by constructing the linearized model was proposed. After each iteration they were defined as

$$\begin{cases} \Delta\boldsymbol{K} = \dfrac{\Delta\boldsymbol{K} + \Delta\boldsymbol{K}^T}{2} \\ \Delta\boldsymbol{M} = \dfrac{\Delta\boldsymbol{M} + \Delta\boldsymbol{M}^{\mathrm{T}}}{2} \end{cases} \tag{10}$$

where superscript T denoted transpose.

The iterative procedure was completed when the residual vector satisfied the error tolerance. The residual vectors were defined as the combination of eigenfrequency and mode shapes

$$\varepsilon = \begin{bmatrix} \varepsilon^{\omega} \\ \varepsilon^{m} \end{bmatrix} \leq err \tag{11}$$

where err was the error tolerance; ε was the residual vector; ε^{ω} and ε^{m} were the eigenfrequency residual vectors and mode shape residual vectors, respectively, which were expressed as follows

$$\varepsilon^{\omega}(i) = \frac{|\omega_i^* - \widetilde{\omega}_i|}{|\omega_i^*|} \tag{12}$$

$$\varepsilon^{m}(i) = 1 - \mathrm{MAC}(i) \tag{13}$$

$$\mathrm{MAC}(i) = \frac{\{\widetilde{\emptyset}_i{}^T \phi_i^*\}}{\left(\{\widetilde{\emptyset}_i\}^T\{\widetilde{\emptyset}_i\}\right)\left(\{\phi_i^*\}^T\{\phi_i^*\}\right)} \tag{14}$$

MAC was defined to quantify the consistency of two mode shapes (Pastor *et al.* 2012), where $\widetilde{\omega}_i$ were the ith eigenfrequency from the tuned ROM at each iteration; $\widetilde{\emptyset}_i$ were the ith mode shapes from tuned ROM at each iteration.

However, the governing equations in Eq. (7) were usually underdetermined and the singular values of matrix **A** may gradually decay to zero. Consequently, the solution to Eq. (7) may be unstable. For such ill-conditioned problems, the Tikhonov regularization was the most popular approach to obtain a meaningful approximate solution (Wang *et al.* 2012, Friswell *et al.* 2001). In its simplest form, the Tikhonov regularization was used to replace the solution of Eq. (7) by solving the following minimization problem

$$min\{\|\boldsymbol{b} - \boldsymbol{A}x\|^2 + \lambda^2\|x\|^2\} \tag{15}$$

where λ was a positive constant and $\|\cdot\|$ donated the norm of a vector or matrix.

When substituting the Eq. (9) into Eq. (15), the solutions of $\|x\|^2$ and residual norms $\|r\|^2$can be given as follows (Hansen *et al.* 2001)

$$\|x\|^2 = \sum_{i=1}^{n} f_i^2 \frac{(u_i^T b)^2}{\sigma_i^2} \tag{16}$$

$$\|r\|^2 = \|\boldsymbol{b} - \boldsymbol{A}x\|^2 = \sum\nolimits_{i=1}^{n} (1 - f_i)^2 \, (u_i^T b)^2 \tag{17}$$

where $f_i = \frac{\sigma_i^2}{\sigma_i^2 + \lambda^2}$;

Note that $\|x\|^2$ and $\|r\|^2$ were both the functions of λ. This regularization method was closely related to the optimization of multi-objective functions, and it sought a suitable regularization parameter λ to keep the balance between $\|x\|^2$ and $\|r\|^2$. If λ was too small, then it would be the original ill-posed problem, but if λ was too large then the problem would have little connection with the original problem. A useful tool to select an appropriate regularization parameter was the L-curve (Rezghi *et al.* 2009). When seeking the optimal λ, the solution to Eq. (7) can be formulated as

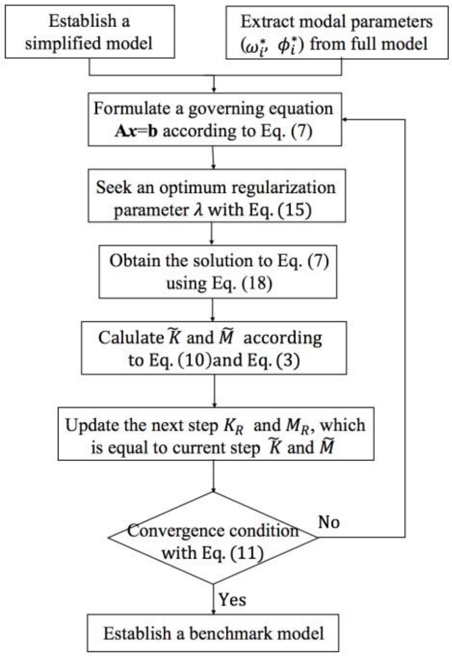

Fig. 5 Flowchart of the iterative matrix method with regularization

$$x = \sum_{i=1}^{n} \frac{u_i^T b}{\sigma_i^2 + \lambda^2} \tag{18}$$

The regularization should be applied at each iteration, but the values of regularization parameters were difficult to determine during the iterations because the corner of the L-curve sometimes disappeared. For convenience, the regularization parameter was set from the first iteration until it converged. To sum up, the iterative matrix method with regularization was shown in Fig. 5.

3.2 Model tuning result

Based on the proposed method in Section 3.1, the model tuning procedure was conducted using the first 9 full model frequencies and modal shapes to seek the optimum regularization parameters. As seen in Fig.6, the point with maximum curvature at the corner of L-curve can be considered as a balance between $\|x\|^2$ and $\|r\|^2$, so the optimum value was taken as 0.77.

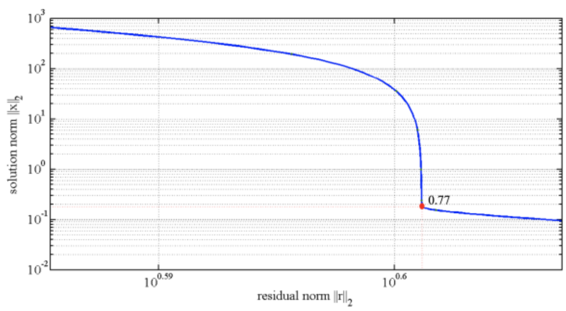

Fig. 6 L-curve for optimum regularization parameters

Table 3 Comparison of the modal parameters between full model and tuned ROM

Order	Full model frequency/Hz	Tuned ROM frequency/Hz	MAC
1	0.108	0.108	1
2	0.110	0.110	1
3	0.140	0.139	0.988
4	0.296	0.295	0.988
5	0.310	0.309	0.991
6	0.352	0.353	0.989
7	0.576	0.577	0.990
8	0.599	0.599	0.993
9	0.622	0.621	0.985

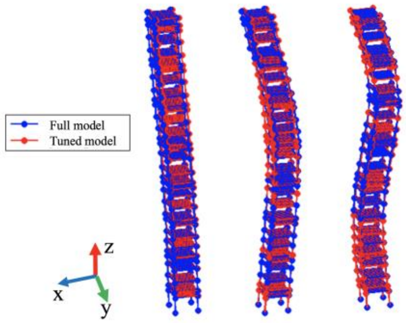

(a) First three modes in X direction

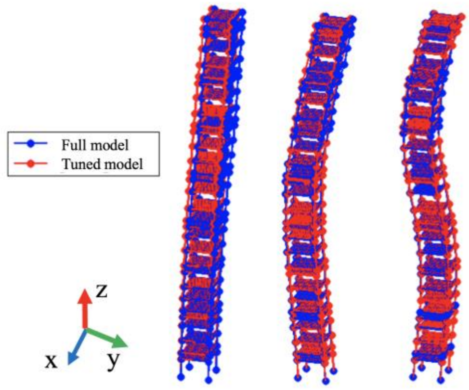

(b) First three modes in Y direction

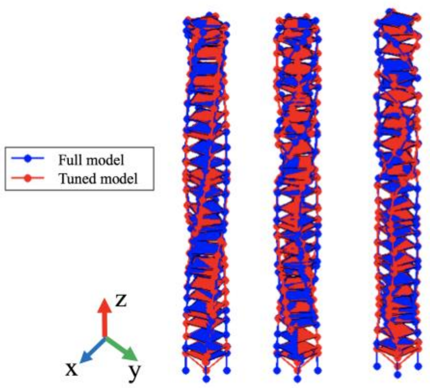

(c) First three torsional modes

Fig. 7 Comparison of the mode shapes from full model and tuned ROM

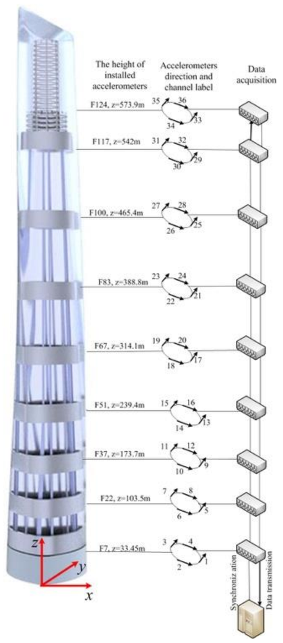

Fig. 8 Vertical layout information of accelerometers

The tuned result of natural frequencies was summarized in Table 3. It was seen that the tuned natural frequencies were much close to those of the full model. The MAC values between the tuned mode shapes and the corresponding ones obtained from the full model were also shown in this table. It was seen that they were almost equal to 1, indicating that the two mode shapes were nearly the same. The first nine mode shapes were shown in Fig. 7 and they were reasonable. For the purpose of intuitive comparison, the nodes and elements in the mode shapes of the full model corresponding to those nodes and elements in the tuned ROM were selected as displayed in Fig. 7. Therefore, the tuned ROM can be regarded as a SHM-oriented model, which can be used to fast analysis and predict the vibration response of this structure in the future analysis.

4. Long-term SHM for Shanghai Tower

4.1 Description of structure health monitoring system for Shanghai Tower

A sophisticated SHM system, which consisted of more than 400 sensors of 11 different types, was designed to monitor the performance of the Shanghai Tower during its serviceability (Su *et al.* 2013). In various sensors, a series of accelerometers were used to record the dynamic response of structure and identify the modal parameters. They can also provide reliable measurement for static and dynamic displacement together with GPS. There were thirty-six accelerometers equipped with this structure as shown in Fig. 8. According to the mechanical characteristics of structure and access to the data acquisition units, they were installed at eight strengthen floors. The layout of typical

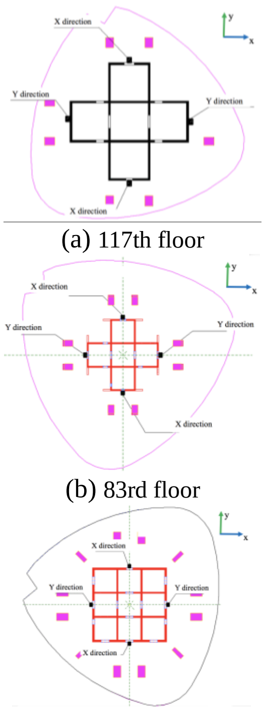

(a) 117th floor

(b) 83rd floor

(c) 51st floor

Fig. 9 Plan layout information of typical floors

floor were shown in Fig. 9. There were four uniaxial accelerometers installed on the shear wall of the core tube at each floor. Two were used to measure the horizontal vibration along the x axis of the core tube and the other two were used to measure the vibration of the y axis of the core tube.

4.2 Dynamics characteristics monitoring of structure in different construction stages

To evaluate the structural performance and control the construction errors within the allowable limit, a series of ambient vibration tests were carried out to monitor the structural response under construction (Zhang *et al.* 2016b). An overview of the structures at different construction stages and the corresponding FE models were shown in Fig. 10. In each test, two uniaxial piezoelectric accelerometers with a frequency range of 0.05 to 500 Hz were used, and the sampling frequency was set to 20Hz. Data were collected for at least 30 minutes during each test. For all 10 ambient tests, two typical operational modal analysis techniques, i.e., the Peak Picking (PP) (Clough, 1995) method and Stochastic Subspace Identification (SSI) (Peeters and Roeck, 1999), were used to identify modal parameters. The identified natural frequencies of structure at different construction stages were shown in Fig. 11, each legend was illustrated here: PP denoted the natural frequencies identified by PP method; SSI denoted the natural frequencies identified by SSI method; ETABS denoted the natural frequencies obtained from the FE model. It was seen that the natural frequencies decreased with the increasing of the structural height.

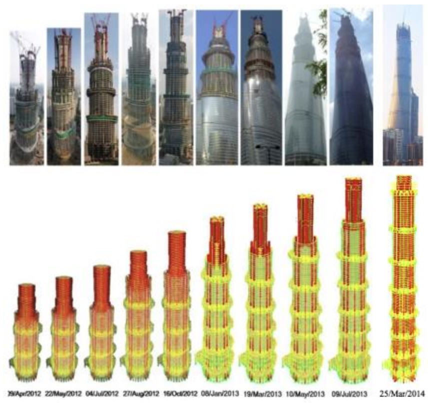

Fig. 10 Overview of Shanghai Tower at different construction stages and corresponding FE models (Zhang *et al.* 2016b)

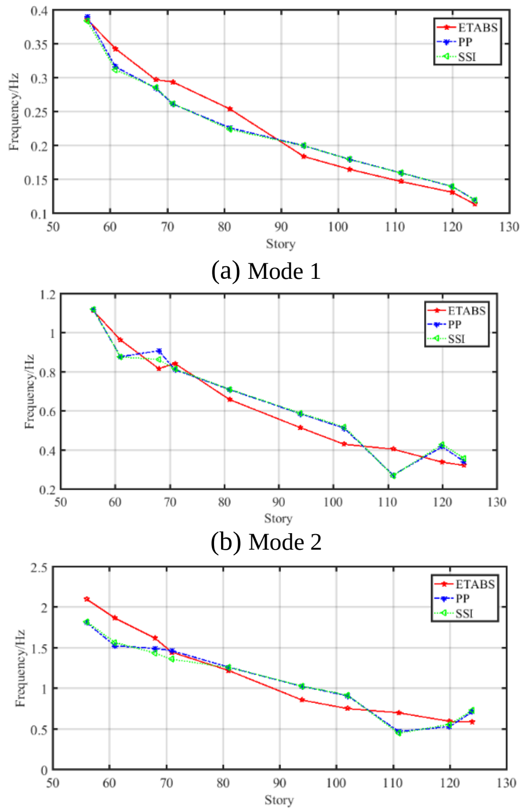

(a) Mode 1

(b) Mode 2

(c) Mode 3

Fig. 11 Identified mode frequencies at different construction stages

Comparing the natural frequencies identified by the PP method and SSI method, the maximum relative errors were 1.6%, 5.2% and 7.8% for the first-mode, second-mode and third-mode frequency respectively. It was stated that the identified result with these two methods were reliable. It was also noticed that the second and third frequency in the 112th story were lower than those frequencies in the 120th and 124th floors. This result may be caused by the noise of some machines during the test. Comparing the identified result with the FE model, the relative errors (except the 112th floor) were up to 12.8%, 20.2% and 17.9% for the

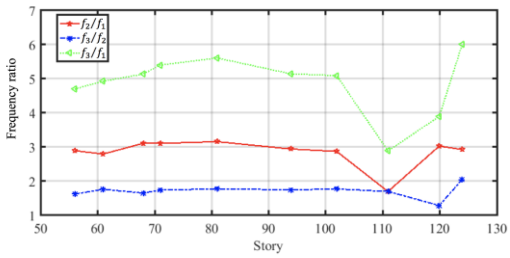

Fig. 12 The first three frequency ratios versus the number of story

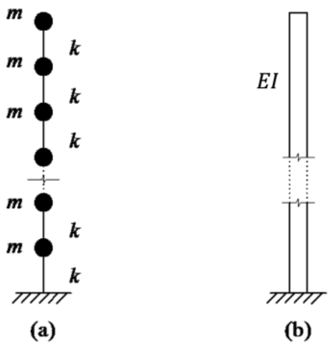

Fig. 13 Idealized simple models: (a) MDOF model and (b) a continuous model of Bernoulli-Euler beam

first-mode, second-mode and third-mode frequency respectively. It may be due to the simplified assumptions and construction live load. For example, the supercolumn embeds steel plate in practical, however, when establishing the FE model, an equivalent stiffness method was adopted to simulate this component.

To investigate the relationship between the natural frequencies and the number of stories, the ratios of the second modal frequencies to the first modal frequencies (f_2/f_1), the third modal frequencies to the second modal frequencies (f_3/f_2) and the third modal frequencies to the first modal frequencies (f_3/f_1) with respect to the number of stories were plot in Fig. 12. It can be observed that f_2/f_1 was in the range of 2.7 to 3.2, f_3/f_2 was in the range of 1.6 to 2.1, and f_3/f_1 was in the range of 4.6 to 6.1. As the identified result of 112th story and 120th story may contain noise pollution, these two stories were not taken into consideration. These interesting observation can be explained from theoretical analysis. As the Shanghai Tower was a combined system of mega-frame core-wall structural system, it can be regarded as a combination of a shear structure and a flexural structure. For a shear structure, it can be simplified to a multi-degree of freedom (MDOF) model, as shown in Fig. 13(a), and free vibration of the MDOF model was governed by the following equation

$$\mathbf{M}\ddot{u} + \mathbf{K}u = 0$$

$$\text{where } \mathbf{M} = \begin{bmatrix} m & 0 & \cdots & 0 \\ 0 & m & \cdots & 0 \\ \vdots & \vdots & \ddots & \vdots \\ 0 & 0 & 0 & m \end{bmatrix},\ \mathbf{K} = \begin{bmatrix} 2k & -k & \cdots & 0 \\ -k & 2k & \cdots & 0 \\ \vdots & \vdots & \ddots & \vdots \\ 0 & 0 & \cdots & 2k \end{bmatrix}; \quad (19)$$

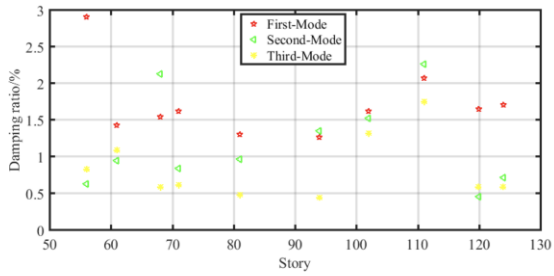

(a)

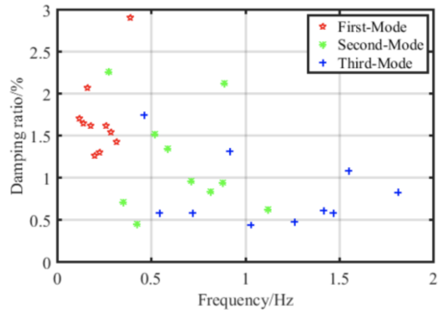

(b)

Fig. 14 First three damping ratios identified: (a) The first three damping ratios versus number of story and (b) The first three damping ratios versus the corresponding frequency

The nature frequencies can be calculated from the eigenvalue equation, which was expressed as

$$\det[\mathbf{K} - \omega^2\mathbf{M}] = 0; \quad (20)$$

Solving the Eq. (20), the ratios of f_2/f_1, f_3/f_2 and f_3/f_1 were 3.0, 1.67 and 5.0, respectively.

For a flexural structure, it can be idealized to a continuous model of Bernoulli-Euler beam (Fig. 13(b)), and the free vibration was governed by

$$(EIu'')'' + \rho A u = 0 \quad (21)$$

where E was elastic modulus; I was moment of inertia; ρ was density; A was area

The nature frequencies derived from Eq. (21) were given by (Craig *et al.* 2006)

$$\omega_1 = \frac{3.516}{L^2}\left(\frac{EI}{\rho A}\right)^{1/2},\ \omega_2 = \frac{22.03}{L^2}\left(\frac{EI}{\rho A}\right)^{1/2},\ \omega_3 = \frac{61.07}{L^2}\left(\frac{EI}{\rho A}\right)^{1/2} \quad (22)$$

It can be calculated that the ratios of $f_2/f_1 = 6.27$, $f_3/f_2 = 2.8$, and $f_3/f_1 = 17.55$. As the idealized flexural model and the shear model were two extreme models for Shanghai Tower. The theoretical frequency ratios of f_2/f_1, f_3/f_2 and f_3/f_1 should be approximately fell into the range of 3.0 to 6.27, 1.67 to 2.80, and 5.0 to 17.55, respectively. Compared with the identification result from ambient vibration tests, it can be seen that most of them lied in the theoretical range.

For tall buildings, damping was another important topic attracting many researchers' interest (Smith 2007, Spence *et al.* 2014a). The damping ratios at different construction stages of this supertall building were estimated with a half-power bandwidth method (Papagiannopoulos and Hatzigeorgiou 2011), as shown in Fig. 14(a). The damping-frequency relationship was investigated in Fig. 14(b). It can be observed that the damping ratio showed great variation. No obvious trend can be found. One possible reason was that the identification of this quality had larger uncertainty (Zhang *et al.* 2016b). In general, various researches were tried to investigate the possible trends for damping. For example, Jeary (1986) proposed a simple linear formulation to describe the relation between damping and frequency. A more complicated relationship was proposed by Lagomarsino (Lagomarsino, 1993), i.e., $\xi = \frac{\beta_1}{f} + \beta_2 f$, where β_1 and β_2 were constant. However, damping had many sources of varying complexity. The excitation amplitude (Aquino and Tamura, 2011) and damping estimation approaches also had significantly influence in the identification result. Currently, the damping characteristic was mainly investigated from full-scale measurement, as many structure health monitoring programs had helped to establish a number of damping databases over the years (Davenport *et al.* 1986, Satake *et al.* 2003, Spence *et al.* 2014b). The damping value from field measurement at different construction stages presented in this paper also provided an important database for further investigation.

3.2 Model tuning result

Shanghai Tower was completed in March 2016, and was ranked as the second tallest building in the world until now. For such a large-scale structure, assessing its dynamic characteristics can be helpful to understand the real performance of the structure. In this study, the data recorded by the SHM system from 20:00pm to 21:00pm on 10 August 2017 were used for the operational modal analysis.

Based on the FE model analysis, the natural frequencies of interest were less than 1 Hz, so the raw acceleration responses were filtered by a low-pass filter with a cut-off frequency of 2 Hz. This can improve the quality of spectrums analysis from the structural response when using the analysis methods in this paper. Two different algorithms, i.e., enhanced frequency domain decomposition (EFDD) (Brincker *et al.* 2001) and SSI (Peeters and Roeck 1999) were used to identify the modal parameters of this structure, where the SVD spectrum and stabilization diagram of SSI were shown in Figs. 15 and 16, respectively. The estimation results from two different methods and the FE model were listed in Table 4. It can be found that the fundamental frequency of this structure was 0.11Hz and the corresponding period was 9.35s, which exceeded 6s limitation of design response spectrum in the China Code of Seismic Design (GB50011-2010, 2010). Since this structure had a symmetrical layout, the natural frequencies were very close in both x and y directions. The natural frequencies identified by two methods were very close, while the damping ratios had a relatively large difference. This demonstrated again that the identification of damping ratios was dependent on the identified algorithm.

Compared with the results from ETABS, the identified results from two independent methods were a little smaller at low frequencies, while they were larger at higher frequencies. This may be attributed to some unknown or uncertain factors in practical structure, for instant, simplified modelling assumptions, material properties and boundary conditions. These identified modal properties

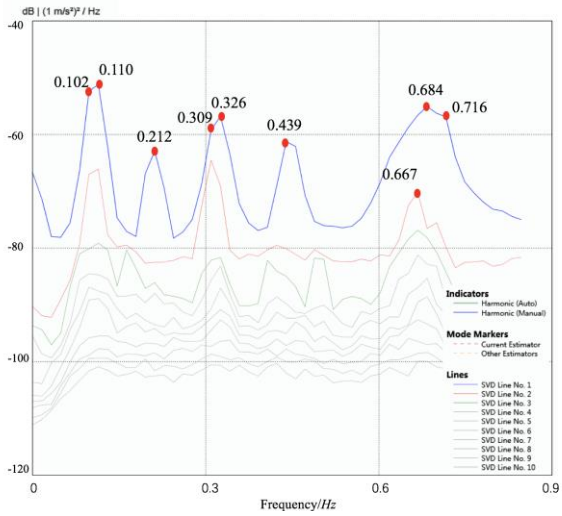

Fig. 15 Singular value decomposition spectrum

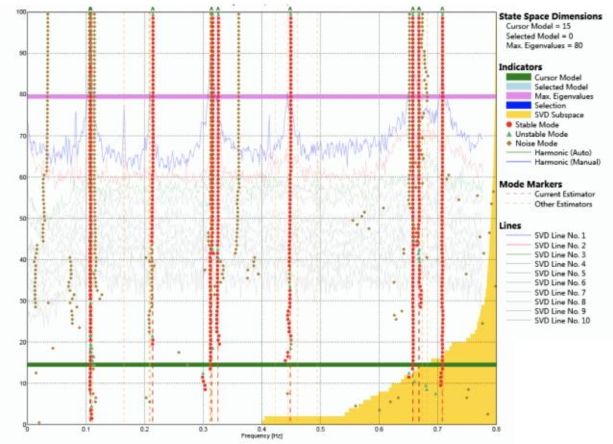

Fig. 16 Stabilization diagram of SSI

Table 4 Modal parameters determined by FE model and two identification methods

Mode	ETABS	EFDD		SSI		Direction
	f/Hz	f/Hz	ξ/%	f/Hz	ξ/%	
1	0.108	0.102	2.81	0.107	2.73	Y
2	0.11	0.11	2.59	0.108	1.97	X
3	0.14	0.212	3.07	0.214	2.91	Torsion
4	0.296	0.309	2.89	0.314	1.08	Y
5	0.31	0.326	2.01	0.325	1.82	X
6	0.352	0.439	1.72	0.448	0.66	Torsion
7	0.576	0.667	1.02	0.658	0.73	Y
8	0.599	0.684	1.22	0.667	2.01	X
9	0.622	0.716	0.94	0.709	0.95	Torsion

were useful to check or update FE model and to tune vibration control devices installed on the tower. Furthermore, a better baseline model of the tower can be developed as a reference to check the evolution of its dynamic characteristics. The mode shapes of the first 9 modes were shown in Fig. 17, including three translational modes in the X and Y directions and three torsional modes, which were all reasonable. From the mode shapes, it can be seen that although the architectural appearance of this structure looked like a rotating shape, the dynamic characteristic was relatively regular. These results were also consistent with the study in Zhang *et al.* (2018).

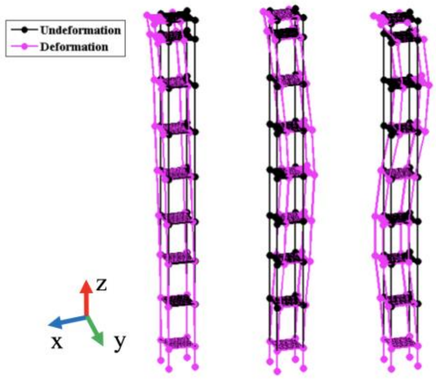

(a) First three modes in X direction

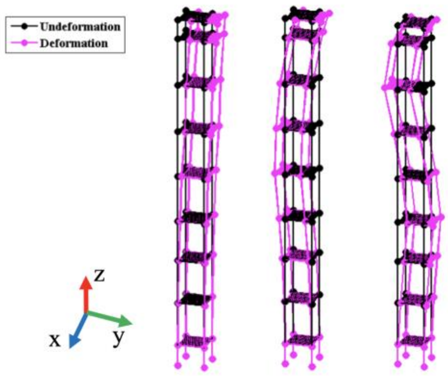

(b) First three modes in Y direction

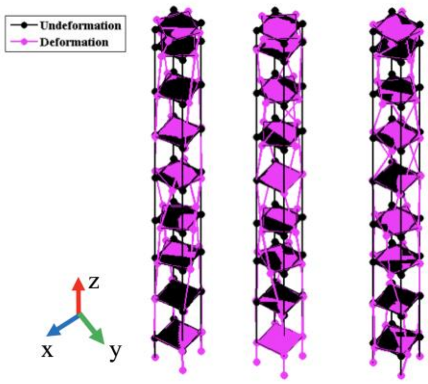

(c) First three torsional modes

Fig. 17 Mode shapes identified by EFDD method

5. Conclusions

This paper presented the work on the development of a benchmark reduce-order model for Shanghai Tower and the investigation of dynamic characteristics of the structure from field measurement. The main conclusions can be summarized as follows:

- A reduced-order model for Shanghai Tower was successfully generated from the full model, consisting of 31 elements. An iterative matrix method with regularization was proposed to tune the system parameters. The tuned reduced-order model had a good consistency with the full model, which can be used as a SHM-oriented model.
- Long-term monitoring of dynamic characteristics in different construction stages had been investigated. The identified results showed that the frequency ratios of f_2/f_1, f_3/f_2 and f_3/f_1 lied in a certain range. These ranges were discussed from the aspect of the structure system, in which the system was regarded as a combination of a shear structure and a flexural structure. The damping ratio had a much larger dispersion than the natural frequency. This field database provided a valuable reference for further analysis.
- A field measurement was conducted during its service. The identified results had a good agreement with the finite element model. Damping ratio was difficult to identify and some uncertainties would be exist. Bayesian method could provide a rigorous way to quantify the uncertainties (Au 2017) and it can be used for the future analysis of this building. Finally, the identified modal parameters would be useful to check or update finite element model and examine the dynamic characteristics evolution in the future.

Acknowledgments

This paper is funded by the National Natural Science Foundation of China (grant nos. 51878484, 51508407), the Fundamental Research Funds for the Central Universities (22120180315), the Application for Collaborative Research Project under International Joint Research Laboratory of Earthquake Engineering (TMGFXK-2015-002-2), the Interdisciplinary Cooperation Foundation for the Peak Discipline of Civil Engineering at Tongji University. The financial support is gratefully acknowledged. The authors would like to thank Prof. Xilin Lu and Prof. Qilin Zhang from Tongji University and the building owners of the Shanghai Tower, for providing supports in the whole research.

References

Abdelrazaq, A., Amp, H. and Camp, S. (2012), “Validating the structural behavior and response of Burj Khalifa: Full scale structural health monitoring programs”, *Build. Struct.*, **44**(5), 87-97.

Amabili, M., Sarkar, A. and Paidoussis, M.P. (2003), “Reduced-order models for nonlinear vibrations of cylindrical shells via the proper orthogonal decomposition method”, *Fluid. Struct.*,

18(2), 227-250.
Aquino, R. E. and Tamura, Y. (2011), "Damping based on EPP spring models of stick-slip surfaces", *Proceedings of the International Conference on Wind Engineering*.
Au, S.K. (2017), *Operational Modal Analysis Modeling, Bayesian Inference, Uncertainty Laws*. Springer.
Au, S.K. and Zhang, F.L. (2016), "Fundamental two-stage formulation for Bayesian system identification, Part I: general theory", *Mech. Syst. Signal Pr.*, **66-67**, 31-42.
Au, S.K., Zhang, F.L. and To, P. (2012), "Field observations on modal properties of two tall buildings under strong wind". *J. Wind Eng. Ind. Aerod.*, **101**(101), 12-23.
Brincker, R., Zhang, L. and Andersen, P. (2001), "Modal identification of output-only systems using frequency domaindecomposition", *Smart Mater. Struct*., **10**(3), 44
Cao, L. and Li, C. (2019), "Tuned tandem mass dampers-inerters with broadband high effectiveness for structures under white noise base excitations", *Struct. Control Health Monit.*, e2319. https://doi.org/ 10.1002/stc.2319
Chen, W.H., Lu, Z.R., Lin, W., Chen, S.H., Ni, Y.Q., Xia, Y. and Liao, W.Y. (2011), "Theoretical and experimental modal analysis of the Guangzhou New TV Tower", *Eng Struct.*, **33** (12), 3628-3646.
Clough, R.W. and Penzien, J. (1995), *Dynamics of Structures*, Computers & Structures Inc.
Craig, R.R., and Kurdila, A.J. (2006), *Fundamentals of structural dynamics*, John Wiley & Sons.
Davenport, A.G. (1986), "Damping in tall buildings: Its variability and treatment in design", *Building Motion in Wind*, 42-57.
Downs, B. (1980), "Accurate reduction of stiffness and mass matrices for vibration analysis and a rationale for selecting master degrees of freedom", *Mech. Des-T Asme*, **102**(2), 412-416.
Flanigan, C.C. (1991), "Development of the Irs component dynamic reduction method for substructure analysis", *Proceedings of the 32nd Structures, Structural Dynamics, and Materials Conference*.
Friswell, M.I., Mottershead, J.E. and Ahmadian, H. (2001), "Finite-element model updating using experimental test data: parametrization and regularization", *Philos. T. Roy. Soc. A*, **359** (1778), 169-186.
Huang, M.J. (2006), "Utilization of strong-motion records for post-earthquake damage assessment of buildings", *Proceedings of the international workshop on structural health monitoring and damage assessment.*
Hansen, P.H. (2001), "The L-curve and its use in the numerical treatment of inverse problems", invited chapter, in: P. Johnston (Ed.), Computational Inverse Problems in Electrocardiology, WIT Press, Southampton.
GB50011-2010. (2010), *Code for Seismic Design of Building*, Ministry of Construction of the People's Republic of China, Beijing, China.
Guo, Y.L., Kareem, A., Ni, Y.Q. and Liao, W.Y. (2012), "Performance evaluation of Canton Tower under winds based on full-scale data", *J. Wind Eng. Ind. Aerod*., **104**, 116-128.
Jain, S., Tiso, P., Rutzmoser, J.B. and Rixen, D.J. (2017), "A quadratic manifold for model order reduction of nonlinear structural dynamics", *Comput. Struct.*, **188**, 80-94.
Jeary, A.P. (1986), "Damping in tall buildings-a mechanism and a predictor", *Earthq. Eng. Struct.*, **14**(5), 733-750.
Kerschen, G., Golinval, J.C., Vakakis, A.F. and Bergman, L.A. (2005), "The method of proper orthogonal decomposition for dynamical characterization and order reduction of mechanical systems: An overview", *Nonlinear Dynam*., **41**(1-3), 147-169.
Kijewski-Correa, T.L. and Kareem, A. (2003), "The Chicago monitoring project: a fusion of information technologies and advanced sensing for civil infrastructure". *Struct. Health. Monit. Intell. Infrastr.*, **1**(2), 1003-1010.
Lagomarsino, S. (1993), "Forecast models for damping and vibration periods of buildings", *J. Wind Eng. Ind. Aerod.*, **48**(2-3), 221-239.
Li, B. and Kiureghian, A.D. (2017), "Operational modal identification using variational Bayes", *Mech. Syst. Signal Pr.*, **88**, 377-398.
Ng, C.T. and Au, S.K. (2018), "Mode shape scaling and implications in modal identification with known input", *Eng. Struct.*, **156**, 411-416.
Ni, Y.C., Lu, X.L. and Lu, W.S. (2017), "Operational modal analysis of a high-rise multi-function building with dampers by a Bayesian approach", *Mech. Syst. Signal Pr.*, **86**, 286-307.
Ni, Y.C., Zhang, Q.W. and Liu, J.F. (2019), "Dynamic property evaluation of a long-span cable-stayed bridge (Sutong Bridge) by a Bayesian method", *Int. J. Struct. Stability Dynam.*, **19**(1), 1940010.
Ni, Y.C. and Zhang, F.L. (2016), "Bayesian operational modal analysis of a pedestrian bridge using a field test with multiple setups", *Int. J. Struct. Stability Dynam.*, **16**(8), 1550052.
Ni, Y.C. and Zhang, F.L.(2018), "Fast Bayesian approach for modal identification using forced vibration data considering the ambient effect", *Mech. Syst. Signal Pr.*, **105**, 113-128.
Ni, Y.C. and Zhang, F.L.(2019), "Fast Bayesian approach for modal identification from seismic response data", *Comput. Struct.*, **212**, 225-235.
Ni, Y.C., Zhang, F.L., Lam, H.F. and Au, S.K. (2016), "Fast Bayesian approach for modal identification using free vibration data, Part II—Posterior uncertainty and application", *Mech. Syst. Signal Pr.*, **70**, 221-244.
Ni, Y.Q., Xia, Y., Liao, W.Y. and Ko, J.M. (2009), "Technology innovation in developing the structural health monitoring system for Guangzhou New TV Tower", *Struct. Control Health*, **16**(1), 73-98.
Ni, Y.Q., Xia, Y., Lin, W., Chen, W.H. and Ko, J.M. (2012), "SHM benchmark for high-rise structures: a reduced-order finite element model and field measurement data", *Smart Struct. Syst.*, **10**(4-5), 411-426.
Osmancikli, G., Ucak, S., Turan, F.N., Turker, T. and Bayraktar, A. (2012), "Investigation of restoration effects on the dynamic characteristics of the Hagia Sophia bell-tower by ambient vibration test", *Constr. Build. Mater.*, **29**, 564-572.
Peeters, B. and Roeck, G.D. (1999), "Reference-based stochastic subspace identifitcation for output-only modal analysis", *Mech. Syst. Signal Pr.*, **13**(6), 855-878.
Papagiannopoulos, G.A. and Hatzigeorgiou, G.D. (2011), "On the use of the half-power bandwidth method to estimate damping in building structures", *Soil Dyn. Earthq. Eng.*, **31**(7), 1075-1079.
Pastor, M., Binda, M. and Harcarik, T. (2012), "Modal assurance criterion", *Modell. Mech. Mechatron. Syst.*, **48**, 543-548.
Rahmani, M. and Todorovska, M.I. (2015), "Structural health monitoring of a 54-story steel-frame Building using a wave method and earthquake records", *Earthq. Spectra.*, **31**(1), 501-525.
Rezghi, M. and Hosseini, S.M. (2009), "A new variant of L-curve for Tikhonov regularization", *Comput. Appl. Math.*, **231**(2), 914-924.
Rutzmoser, J.B., Rixen, D.J., Tiso, P. and Jain, S. (2017), "Generalization of quadratic manifolds for reduced order modeling of nonlinear structural dynamics", *Comput. Struct*., **192**, 196-209.
Satake, N., Suda, K., Arakawa, T., Sasaki, A. and Tamura, Y. (2003), "Damping Evaluation Using Full-Scale Data of Buildings in Japan", *J. Struct. Eng.*, **129**(4), 470-477.
Smith, R.J. and Willford, M.R. (2007), "The damped outrigger concept for tall buildings", *Struct. Des. Tall Spec.*, **16**(4), 501-517.

Su, J.Z., Xia, Y. and Chen, L. (2013), "Long-term structural performance monitoring system for the Shanghai Tower", *J. Civil Struct. Health. Monit.*, **3**(1), 49-61.

Spence, S.M.J., Bernardini, E., Guo, Y., Kareem, A. and Gioffrè, M. (2014a), "Natural frequency coalescing and amplitude dependent damping in the wind-excited response of tall buildings", *Probabilist. Eng. Mech.*, **35**(6), 108-117.

Spence, S.M.J. and Kareem, A. (2014b), "Tall buildings and damping: a concept-based data-driven model", *J. Struct. Eng.*, **140**(5),

Wang, J. and Yang, Q.S. (2012), "Modified tikhonov regularization in model updating for damage identification", *Struct. Eng. Mech.*, **44**(5), 585-600.

Xiong, H.B., Cao, J.X. and Zhang, F.L. (2018), "Inclinometer-based method to monitor displacement of high-rise buildings", *Struct. Monit. Maint.*, **5**(1), 111-127.

Yin, T., Jiang, Q.H. and Yuen, K.V. (2017), "Vibration-based damage detection for structural connections using incomplete modal data by Bayesian approach and model reduction technique", *Eng. Struct.*, **132**, 260-277.

Yi, J., Zhang, J.W. and Li, Q.S. (2013), "Dynamic characteristics and wind-induced responses of a super-tall building during typhoons", *J. Wind Eng. Ind. Aerod.*, **121**, 116-130.

Yi, T.H., Li, H.N. and Gu, M. (2013), "Recent research and applications of GPS-based monitoring technology for high-rise structures", *Struct. Control Health.*, **20**(5), 649-670.

Zhang, F.L., Ni, Y.Q., Ni, Y.C. and Wang, Y.W. (2016a), "Operational modal analysis of Canton Tower by a fast frequency domain Bayesian method", *Smart Struct. Syst.*, **17** (2), 209-230.

Zhang, F.L., Xiong, H.B., Shi, W.X. and Ou, X. (2016b), "Structural health monitoring of Shanghai Tower during different stages using a Bayesian approach", *Struct. Control Health.*, **23**(11), 1366-1384.

Zhang, F.L., Ni, Y.C. and Lam, H.F. (2017). "Bayesian structural model updating using ambient vibration data collected by multiple setups", *Struct. Control Health.*, **24**(12), e2023.

Zhang, F.L., Ventura, C.E., Xiong, H.B., Lu, W.S., Pan, Y.X. and Cao, J.X. (2018), "Evaluation of the dynamic characteristics of a super tall building using data from ambient vibration and shake table tests by a Bayesian approach", *Struct. Control Health.*, **25**(2), e2121.

BS